INT-148/88 August 1988

A Plasma Current Profile Diagnostic Using the Frequency Splitting of the Axisymmetric Magnetoacoustic Wave Resonance

G.G. Borg

ABSTRACT

In the presence of finite plasma current, the axisymmetric $(m = 0)$ magnetoacoustic wave resonance exhibits a frequency splitting for finite n between $n = \pm|n|$ travelling waves. Calculations are presented which demonstrate that $\Delta(1/f)$ the difference between the inverse resonant frequencies, is directly proportional to known moments of the plasma current profile and, in the limit where the radial wavenumber is much larger than the parallel wavenumber, is independent of the plasma mass density and the plasma mass density profile. Some aspects of the implementation of a current profile diagnostic based on the excitation of these resonances are also considered.

1. INTRODUCTION

Several techniques for measuring parameters derived from the plasma current profile have been proposed and tested.

The simplest, presently available on TCA, is the measure of $\Lambda = \beta_p + l_i/2$ provided by the vertical field. In this case the plasma internal inductance l_i can be obtained by a separate measurement of β_p, poloidal beta. Changes in l_i can be indirectly inferred by comparing the temporal evolution of Λ with that of β_{pL} obtained from the diamagnetic loop.

The use of the fundamental and harmonics of the $(n, m) = (0, 0)$ magnetoacoustic resonance impedance has been proposed to obtain unambiguous information on the current profile. [1] An experiment [2] restricted to the fundamental resonance, however, has shown little sensitivity of the magnetoacoustic resonance to the plasma current.

Eigenmode resonances of the Discrete Alfvén wave (DAW) have also been considered [3] as a

possible current profile diagnostic. To date, however, it is not known precisely what measure of the current profile is provided by the DAW eigenfrequency. In fact, more than one profile may lead to the same frequency. The DAW frequency does however lead to a fairly precise parameterisation of l_i and $q(a/2)$ but a major disadvantage remaining is that the frequency also depends critically on the plasma mass density and its profile, neither of which can be measured.

Several methods ([4], [5], [6]) of measuring the q-profile directly have been proposed and tested. Despite the success of these methods however, their complexity emphasizes the demand for a system which is simple to set up and provides a simply interpretable result. In this report, we explore the properties of the axisymmetric $|n| \neq 0$ magnetoacoustic wave with a view to an exploitation of its resonant frequencies as a plasma current profile diagnostic.

Frequency splitting of magnetoacoustic wave resonances has previously been observed using magnetic probes ([7], [8]) and collective scattering [9]. In these cases, high power RF was employed at a single frequency while a density scan swept the spectrum. Previous calculations have shown that the frequency splitting is given by [8],

$$\left(\frac{\Delta\rho}{\rho}\right)_\omega = \frac{2nma^2}{3R^2\langle q\rangle} \qquad 1)$$

where a, R are the minor, major radius respectively, $\langle q\rangle$ the average value of the safety factor and $(\Delta\rho/\rho)_\omega$ the fractional density splitting at constant frequency. Terms of order n^2a^2/R^2 have been neglected with respect to unity in equation 1).

From equation 1) knowledge of the density is absolutely necessary in order to estimate $\langle q\rangle$. In addition, equation 1) predicts no splitting for $m = 0$. We will see in the next section that equation 1) arises from the redefinition of k the toroidal wavenumber, to $k_\parallel$ the parallel wavenumber, when a finite poloidal field is included in the simple MHD model. The redefinition of k however is not the only effect of a finite plasma current on the magnetoacoustic wave. We shall see that equation 1) is substantially modified when the $\underline{J} \times \underline{b}$ force of the current density $\underline{J}$, acting on the wavefield $\underline{b}$, is taken into consideration.

No previous attempt has been made to compare equation 1) with experimental results. In addition, to the best of the author's knowledge, no experimental results on the excitation of the $|n| \neq 0$, $m = 0$ magnetoacoustic resonance in a tokamak have ever been published.

The structure of this report is as follows. In section 2), the analytical theory of the magnetoacoustic resonance splitting in a homogeneous plasma is discussed and a simple formula is derived expressing the inverse frequency splitting $\Delta(1/f)$ in terms of the constant current density.

In section 3) numerical calculations relevant to TCA are presented which test the predictions of the simple formula, examine the effects of profiles and generalize the simple formula to the case of an inhomogeneous plasma.

In section 4), some aspects concerning the implementation of a current profile diagnostic are considered.

2. THE MAGNETOACOUSTIC RESONANCE IN A HOMOGENEOUS CURRENT CARRYING PLASMA

Appert et al. [10] have considered the spectrum of waves in a plasma cylinder including the effects of finite frequency and plasma current. Using their equations 1) and 2) one obtains the following Bessel equation and dispersion relation for the case of a homogeneous plasma with total field $\underset{\sim}{B}$ and axial current $\underset{\sim}{J}$ [11],

$$\frac{d^2 b_{\parallel}}{dr^2} + \frac{1}{r}\frac{db_{\parallel}}{dr} + \left(k_{\perp}^2 - \frac{m_{\perp}^2}{r^2}\right) b_{\parallel} = 0$$

$$k_{\perp}^2 = \frac{\left(A - k_{\parallel}^2\right)^2 - \left(fA - Dk_{\parallel}\right)^2}{A - k_{\parallel}^2} \qquad -2)$$

$$A = \frac{\omega^2 / V_A^2}{1 - f^2}\,, \quad V_A^2 = B^2/(\mu_0 \rho)\,, \quad f = \omega/\omega_{ci}$$

$$D = \mu_0 J/B\,, \quad m_{\perp} = m - kD/2\,, \quad k_{\parallel} = k + \frac{mD}{2}$$

The dispersion relation is a quadratic in $k_{\parallel}^2$ and therefore has two solutions; the Alfvén wave and the magnetoacoustic (compressional, fast) wave. When there is no vacuum gap between

plasma and wall, application of the boundary condition $b_r = 0$ leads to a discrete spectrum of magnetoacoustic wave modes for all values of (n, m). These radial modes have discrete, fixed values of $k_\perp$ and are labelled by the letter l in increasing order, according to the number of half wavelengths in the radial direction. These modes experience a waveguide cutoff. If there is a vacuum layer [10] then this conclusion is no longer valid for the $m \neq 0$, $l = 1$ modes. These waves propagate as surface waves, have a continuously varying $k_\perp$ and do not experience a waveguide cutoff. We are not concerned with the surface waves in this report.

In the ideal MHD limit, where $f = 0$ and $D = 0$, the magnetoacoustic wave has the following simple dispersion relation,

$$k_\perp^2 + k_{||}^2 = \omega^2 / V_A^2 \qquad 3)$$

In this case the propagation of magnetoacoustic waves in a homogeneous plasma cylinder without a vacuum layer and bounded by a conducting wall is formally analogous to that of electromagnetic waves in a cylindrical waveguide with $C \rightarrow V_A$.

One can attempt a derivation of the frequency splitting by using equation 3) with the definition of $k_{||}$. This approximation is not complete because it ignores the physical effect of the plasma current density on the wavefield, however it does give an insight into the previous work leading to equation 1).

From equation 3) it may be concluded that at a given frequency and $k_\perp$ there are two different resonant densities for each of $+k$ and $-k$. For a given m and l we may write

$$\frac{\omega^2}{V_A^2}\left(1 + \frac{\Delta\rho}{\rho}\right) - \left(\frac{mD}{2} + k\right)^2 = \frac{\omega^2}{V_A^2} - \left(\frac{mD}{2} - k\right)^2$$

We therefore obtain

$$\left(\frac{\Delta\rho}{\rho}\right)_\omega = \frac{mkD}{k_\perp^2}$$

where $k_\perp \gg k$ has been assumed.

In the large aspect ratio limit of a tokamak; $k = n/R$ and $D = \mu_0 J/B_\phi = 2/Rq$ so that,

$$\left(\frac{\Delta\rho}{\rho}\right)_\omega = \frac{2nm}{q k_\perp^2 R^2} \qquad 4)$$

Apart from numerical factors, equation 4) has the same dependencies as equation 1). The validity of equation 4) is questionable not only because of the neglect of the physical effect of plasma current but also, more importantly, because of the neglect of finite frequency. In TCA the magnetoacoustic resonance is in general only observable above the ion cyclotron frequency.

The same derivation applied to equation 2) with $m = 0$ so that $k_\parallel = k$ yields the following formula for the frequency splitting Δf at fixed density;

$$\Delta f = \frac{4nf^2}{q R^2 k_\perp^2} = \frac{2\mu_0 n J f^2}{R B_\phi k_\perp^2}$$

where $n = kR$, $f \gtrsim 1$ and $k_\perp \gg k$ have been assumed. If Δf is sufficiently small with respect to f then,

$$\left|\Delta(1/f)\right| = \frac{4n}{q R^2 k_\perp^2} = \frac{2\mu_0 n J}{R B_\phi k_\perp^2} \qquad 5)$$

Equation 5) correctly includes the effects of finite frequency and plasma current to show that there is a frequency splitting for the case of $m = 0$. The splitting $\Delta(1/f)$ has the following important properties,

(i) $\Delta(1/f)$ is linearly proportional to J. This linearity is intuitively expected to remain valid for the case of an inhomogeneous plasma provided the current profile remains constant. Similarly, division of $\Delta(1/f)$ by the plasma current Rogowski signal provides a measure of the current profile. The precise property of the current profile measured by $\Delta(1/f)$ will be discussed in the next section.

(ii) Since the radial wavenumber, $k_\perp$ is a constant for a given vessel geometry, $\Delta(1/f)$ is not dependent on plasma mass density. On the other hand $\Delta(1/f)$ should depend on the mass density profile. This will also be discussed in the next section.

For the $m = 0$ magnetoacoustic wave in a homogeneous cylindrical plasma bounded by a conducting wall, $b_r \sim J_1(k_\perp r)$ where J_1 is the Bessel function of order unity. The condition $b_r(a) = 0$ thus yields $k_\perp a$ = 3.83, 7.02, 10.2, 13.3 etc for the various radial modes ℓ = 1, 2, 3, 4 etc and a is the minor radius. Substituting the TCA values a = 0.18, R = 0.61 m into equation 5 and taking $\bar{q} \simeq 2$, we obtain $\Delta(1/f)$ = 0.012 n and 0.003 n respectively for ℓ = 1 and 2. The condition $k_\perp >> k$ is satisfied for $|n| << 12$ and $|m| << 24$ in each case.

3. NUMERICAL RESULTS FOR THE CASE OF AN INHOMOGENEOUS PLASMA

A numerical study of the $\Delta(1/f)$ splitting for an inhomogeneous plasma was performed using the cylindrical code ISMENE. These results are necessary in order to reveal the dependence of the splitting on the plasma current and mass density profiles and hence to generalise equation 5). Unless otherwise stated, the TCA parameters of table 1 were used in the study.

Table 1

Plasma Current, I_p	130 kA
Toroidal Field, B	1.51 T
Major Radius, R	0.61 m
Minor Radius, a	0.18 m
Wall Radius, n	0.24 m
T_i (0), T_e (0)	500, 800 eV
Electron density, $n_e(0)$	7.5×10^{19} m^{-3}
Electron density profile	$(1-0.853\ (r/a)^2)^{1.2}$
with Deuterium filling gas.	
Current density profile,	$(1 - (r/a)^2)^2$

In Fig. 1, the spectrum of calculated resonances for $m = 0$, $|n|$ = 1, 2, 4, 8 and 16, ℓ = 1, 2 and 3 are plotted for the above conditions as a function of frequency between 10 and 30 MHz. The fundamental cyclotron frequency at 11.6 MHz and its first harmonic are shown as vertical dotted lines. The frequency splitting for the different signs of n and the increase in the magnitude of the splitting with $|m|$ is clearly evident in the figure; the $n < 0$ resonance having the lower frequency in each case. The broken curves connect the resonances associated with a given radial mode (ℓ). The Q of the resonances ($\approx 10^5$) are generally quite large.

ISMENE was run as a kinetic code in which TTMP was the main damping mechanism. An anomalous collision frequency of 100 times the Spitzer value was also included to account for possible turbulence enhanced collisions [13], however no effect on wave damping was observed.

3.1 Effect of Plasma Current

The dependence of $\Delta(1/f)$ on plasma current for fixed profiles and conditions otherwise as in table 1, is shown in Fig. 2 for $|n|$ = 1, 2 and 4 and ℓ = 2. It was a general result of the simulations that regardless of the current profile, as long as it is held fixed, $\Delta(1/f)$ is a very linear function of plasma current. This has the advantage that any deviation from a linear dependence on plasma current, checked by comparison with the plasma current Rogowski signal, is evidence of a profile change.

3.2 Effect of Mass Density

The dependence of $\Delta(1/f)$ on equilibrium mass density is shown in Fig. 3. Curves are shown for $|n|$ = 1, 2, 4 and ℓ = 2 as a function of central ion density from 2.5 to 15 x 10^{19} m^{-3} and with density profile constant as in table 1.

Despite the obvious large variations in the individual frequencies f of each resonance, required to satisfy the resonance condition with a changing density, $\Delta(1/f)$ varies negligibly for $|n|$ = 1, 2 and slightly for $|n|$ = 4. In the latter case $k/k_\perp$ = 0.16 and the $k_\perp >> k$ approximation is brought into question.

For the case of $|n|$ = 1, the effect of a mass density profile change has also been examined. In Fig. 3 the effect of varying the exponent of the density profile from 0.40 to 1.60 away from its standard value of 1.2 has been examined for the case of a fixed central density of 7.5 x $10^{19}m^{-3}$ and a fixed average density of 5.11 x $10^{19}m^{-3}$. For $|n|$ = 1 there is clearly no discernible variation in $\Delta(1/f)$. This surprising result must be attributable to the fact that $k_\perp$ is not sensitive to the nature of the profile. Indeed, as shown in Fig. 4 the magnetoacoustic wavefields within the plasma are not very different for the standard profile with a 6 cm vacuum gap than they are for the case of a homogeneous plasma without a vacuum gap. Hence one can imagine a close fitting Bessel function which defines a fairly precise $k_\perp$. This observation ties in with the well known fact that the magnetoacoustic wave propagates at an average Alfvén speed and therefore, to a first approximation, "sees" the plasma as a homogeneous medium. On the other hand, the magnetoacoustic wave with $n > 0$ is affected differently by plasma current to that with $n < 0$, since the transverse wavefield components of $\underset{\sim}{b}$, and hence the forces $\underset{\sim}{J} \times \underset{\sim}{b}$ are oppositely directed.

The insensitivity of $\Delta(1/f)$ to the mass density and its profile is an important asset for a current profile diagnostic.

3.3 The Effect of Plasma Current Profile

Several examples of extreme profile variations are shown in Fig. 5 for $|n| = 1$, $\ell = 2$. Curve a) shows $\Delta(1/f)$ versus I_p at constant current profile as in Fig. 2. Curve b) shows the variation in $\Delta(1/f)$ for $q(o)$ varying from 0.50 to 3.85 with I_p = 100 kA. In this case the exponent in the parabolic profile of Table 1 is varied to keep I_p fixed. Curve c) shows the variation in $\Delta(1/f)$ versus I_p for q (0) = 1. As expected, the variation is less than linear and therefore weaker than that of curve a). This is emphasized in curve d) where curve c) is divided by I_p. The flattening of the current profile at high plasma current is revealed by a decrease in $\Delta(1/f)/I_p$. This sort of behaviour would be expected for example in TCA where $q(o) \rightarrow 1$ at high plasma current.

Having established that $\Delta(1/f)/I_p$ contains information about the current profile we now attempt to find the transformation of the profile on which it depends linearly. It must be emphasized however that, because $\Delta(1/f)/I_p$ is closely constant for a fixed current profile, current profile changes can be detected and, in situations where the current profile can be measured, $\Delta(1/f)/I_p$ can also be calibrated. Hence, for practical purposes knowledge of the transformation is of secondary interest.

One possibility for the transformation is suggested by calculating the propagation speed of the low frequency axisymmetric magnetoacoustic wave in a zero current plasma with a non-uniform mass density. If one considers the ideal MHD equations,

$$-i\omega\rho \underset{\sim}{v} = \underset{\sim}{J} \times \underset{\sim}{B} \qquad 6a)$$

$$\underset{\sim}{E} + \underset{\sim}{v} \times \underset{\sim}{B} = 0 \qquad 6b)$$

and Maxwell's equations, then the equation for a propagating magnetoacoustic wave is given by

$$\nabla^2 \underset{\sim}{b} + \frac{\omega^2}{V_A^2} \underset{\sim}{b} = \mu_0 \nabla \times \underset{\sim}{J}_z + \frac{i\omega\mu_0}{B^2} \cdot (\nabla\rho \times \underset{\sim}{E}) \qquad 7)$$

For the axisymmetric wave, the radial component of equation 7) is

$$\left(\nabla^2 - \frac{1}{r^2}\right) b_r + \frac{\omega^2}{V_A^2} b_r = 0 \qquad 8)$$

Taking $\int_0^a dr\, 2\pi r\, b_r^*$ on both sides one obtains:

$$\langle b_r^* \left(\nabla^2 - \frac{1}{r^2}\right) b_r \rangle + \omega^2 \langle |b_r|^2 / V_A^2 \rangle = 0 \qquad 9)$$

where $\langle X \rangle = \int_0^a 2\pi r X\, dr$. As noted in Fig. 4 the $m = 0$ magnetoacoustic wave within the plasma has approximately a Bessel function character. Hence equation 9) and equation 2) with $m_\perp \rightarrow m = 0$ can be combined to yield;

$$\frac{\omega^2}{V_A^{*2}} = k^2 + k_\perp^2 \qquad 10)$$

where $1/V_A^{*2} = \langle |b_r|^2 / V_A^2 \rangle / \langle |b_r|^2 \rangle$

Note that b_r (approximately a J_1 - Bessel function) is involved in the moment integral for the definition of V_A^* and hence a plasma mass density moment ρ^* . This is natural because the force responsible for the wave is the $\underline{J} \times \underline{B}$ force of equation 6a) and the only component of $\underline{J}$ (J_θ in this limit) is proportional to b_r . Only the plasma in the region of non-zero J_θ provides the inertia restored by $\underline{J} \times \underline{B}$. Equation 10) defines precisely the average density "seen" by the magnetoacoustic wave.

One can invoke the same procedure to infer the moment of the plasma current profile which is describe d by $\Delta(1/f)$. Unfortunately the mathematics in this case does not lead to a simple result. We can however obtain a useful formula with a naive argument along the above lines. In this case the new physics results from the $\underline{J} \times \underline{b}$ term [10] in the momentum equation. Since $\underline{J}$ is approximately parallel to $\underline{B}$, we conclude that b_r , and hence also b_θ at finite frequency, are possible weighting functions, both of which are approximately J_1 Bessel functions.

We therefore define;

$$J^* = \frac{\langle J |b_r|^2 \rangle}{\langle |b_r|^2 \rangle} \qquad 11)$$

which for a uniform J gives $J^* = I_p/\pi a^2$.

We can now rewrite equation 5) as

$$\left|\Delta(1/f)\right| = \frac{2\mu_0 n J^*}{R B_\phi k_\perp^2} \qquad 12)$$

By taking b_r to be simply a J_1 - Bessel function the data of Fig. 5. have been replotted as $\Delta(1/f)$ versus J^* in Fig. 6. In particular calculations were included for a class of flat-top profiles of the form.

$$J(r) = \begin{cases} 1 & : 0 < r < r_0 \\ \exp\left\{-(r-r_0)^2/R_0^2\right\} & : r_0 < r < a \end{cases}$$

The overall point to note from Fig. 6. is that $\Delta(1/f)$ describes very closely the parameter J^*. In other words, $\Delta(1/f)/I_p$ measures the current profile parameter J^*/I_p which is independent of plasma current.

4. A CURRENT PROFILE DIAGNOSTIC BASED ON THE FREQUENCY SPLITTING

In this section we superficially consider some of the practical aspects and problems in the use of the inverse frequency splitting $\Delta(1/f)$ as a current profile diagnostic.

Theoretical considerations have indicated several major advantages. In addition, from a practical point of view, operation above the ion cyclotron frequency permits current profile diagnosis with reduced interference from the harmonics of the Alfvén frequency during Alfvén Wave Heating.

One possible problem to be encountered is that the observed resonance Q is too low to resolve the doublet structure of the peak. Experimental results for $m = 1$ magnetoacoustic wave resonances do in fact show a significant discrepancy between the theoretical $Q \approx 10^5$ and the experimentally observed values for which $Q < 10^3$. The mechanism for the discrepancy is poorly understood however we have already shown that anomalous collisions due to MHD turbulence are not responsible. An additional proposed mechanism is ω_{pi} damping near the edge [14].

In this report calculations were mainly performed for the $m = 0$, $|n| = 1$, $\ell = 2$ mode. For standard conditions of table 1, the frequency splitting $\Delta f / f = 0.008$ can only be amplitude resolved if $Q > 125$.

If Q is too low one may attempt to resolve the doublet by plotting the real and imaginary parts of the wavefield in the complex plane. In this case, the individual resonance frequencies can be inferred from phase rotation during a sweep of the resonance.

An additional problem is that of harmonic cyclotron damping. Experimental results [7] indicate that fundamental ($f = 1$) harmonic damping, occurring when the ion cyclotron layer is in the plasma, completely damps the magnetoacoustic wave and suppresses the resonance. In addition, the resonance peaks are not recovered when the whole plasma is below the ion cyclotron frequency. This precludes the possibility of using the first radial mode in TCA (Fig. 1) except at low densities. Normally no problem is expected at the first harmonic, $f = 2$. However a small amount of Hydrogen impurity in a Deuterium plasma causes significant damping of the resonance when the Hydrogen cyclotron layer is present in the plasma ([7], [14]). A plot of density versus frequency for the first four radial modes of the axisymmetric magnetoacoustic wave is shown in Fig. 7 for TCA conditions. These curves are approximately the same for $|n| = 1$, 2 and 4 and are too coarse to show the splitting. Note that in the $k_\perp >> k$ limit, equation 2) becomes $\omega^2/v_A^2 \simeq k_\perp^2$ and a given resonance occurs at twice the electron density of Hydrogen as Deuterium. The shaded regions correspond to the frequencies for which the Deuterium and Hydrogen cyclotron layers are present in TCA.

If second harmonic cyclotron damping is a problem then in Hydrogen, magnetoacoustic waves up to the fourth radial mode above 30 MHz can be used to measure the current profile. In Deuterium, profile measurements at densities above $\overline{n}_e = 8.0 \times 10^{19} m^{-3}$ can only be made with radial modes higher than the fourth or for frequencies in between the Hydrogen and Deuterium cyclotron frequencies.

Since experimental results on the excitation of the axisymmetric magnetoacoustic wave in a tokamak do not appear to be available, the first step would be a short study of the spectrum to see what mode doublets can be identified and what resonance Qs are obtained over the range of available plasma densities.

A possible experimental arrangement is shown in Fig. 8. A current loop antenna excites the axisymmetric modes. A probe or an additional current loop situated 180^0 toroidally from the antenna detects the toroidal magnetic field component of all axisymmetric, toroidal (n) and radial ($k_\perp$) modes. According to Fig. 1 the low toroidal modes tend to cluster according to radial

order whilst the high toroidal modes at higher frequencies form a dense and uniform spectrum regardless of radial order. Hence low order toroidal mode number selection at low frequencies seems best for identification and tracking. The choice of mode must also be consistent with the condition that $k_\perp \gg k$ to ensure that $\Delta(1/f)$ is independent of plasma mass density.

Once a suitable mode doublet has been located, the operating frequency must be altered to track the doublet as the density evolves. Mode tracking can be performed by feedback ([3], [7]). The system of Fig. 8 allows differentiation between odd and even toroidal modes by their phase with respect to the current in the antenna. Hence a feedback loop using this phase and gated by the amplitude of the resonance peak can be used to selectively lock on odd or even modes.

5. CONCLUSION

Calculations have been presented which show that the inverse frequency splitting $\Delta(1/f)$ between $n = \pm |n|$ modes of the axisymmetric magnetoacoustic wave provides a measure (equation 12) of the moment J^* (equation 11) of the plasma current profile. In the limit where the radial wavenumber, $k_\perp$, is much greater than the toroidal wavenumber, k , $\Delta(1/f)$ measures J^* independently of the plasma mass density and its profile.

The magnetoacoustic wave may also be used to measure the same moment, ρ^*, of the mass density profile [16] (equation 10). Hence the same mode provides a measure of $\frac{\rho^*}{\rho^*}$ from $1/f^2$ and J^* from $\Delta(1/f)$.

Acknowledgement

The author would like to thank Ph. Marmillod and Drs. K. Appert, J. Vaclavik, A. Pochelon and M. Sawley for useful discussions. This work was partly funded by the Fonds National Suisse de la Recherche Scientifique.

REFERENCES

[1] Howell R.B. and Clayton T.F. (1982) Plasma Physics **24**, 1051.

[2] Brennan M.H., McCarthy A. L. and Sawley M. L. (1980) Plasma Physics **22**, 77.

[3] Collins G. A., Howling A.A., Lister J. B. and Marmillod Ph. (1987) Plasma Physics and Controlled Fusion **29**, 323.

[4] McCormick K. et. al. (1985) Proc. 12th European Conference on Controlled Fusion and Plasma Heating Budapest, Vol. 1, p. 199.

[5] Soltwisch H.,Graffman E., Schluter J. and Waidman G. (1984) Proc. Int. Conf. on Plasma Physics Lausanne Vol. 1, p. 499.

[6] Weisen et. al., Phys. Rev. Lett., submitted for publication.

[7] Equipe TFR (1976) Proc. of the Sixth Int. Conf. on Plasma Physics and Controlled Nuclear Fusion Research, Berchtesgaden, (1977) IAEA, Vienna, Vol. 111.

[8] Adam J., Proc. of the Fifth Int. Conf. on Plasma Physics and Controlled Nuclear Fusion Research, Tokyo IAEA, Vienna, Vol. 11.

[9] Park H., Peebles W.A., Luhmann N.C. Jr., Kirkwood R. and Taylor R.J. (1985) Plas. Phys. **27** p. 1195.

[10] Appert K., Vaclavik J. and Villard L. (1984) Phys. Fluids **27**, 432.

[11] Cross R.C. (1983), PP83/7, Internal Report, University of Sydney.

[12] Appert K., Hellsten T., Lutjens H., Sauter O., Vaclavik J. and Villard L. (1987), Proc. 7th Int. Conf. on Plasma Physics, Kiev, Invited Papers, Vol. 2, p. 1230.

[13] Ritz Ch. P. et. al. (1982) Helvetica Physica Acta **55**, 354.

[14] Lallia P. (1975) Nucl. Fusion **15**, 1190.

[15] Borg G.G. and Cross R.C. (1987) Plasma Physics and Contr. Fus. **29**, 681

[16] Brennan M. H., Jessup B. L. and Jones I. R. (1978) Aust. J. Phys. **31**, 477.

FIGURE CAPTIONS

Fig. 1. Spectrum of axisymmetric magnetoacoustic waves in TCA.

Fig. 2. Dependence of $\Delta(1/f)$ on plasma current at fixed profile.

Fig. 3. Dependence of $\Delta(1/f)$ on plasma mass density and its profile. The plasma density profile was varied by changing the exponent α_N.

Fig. 4. Comparison of the radial distribution of the magnetoacoustic wavefield for the case of a homogeneous plasma with no vacuum gap and the case of an inhomogeneous plasma with a 6 cm gap.

Fig. 5. Dependence of $\Delta(1/f)$ for various conditions of plasma current and plasma current profile.

Fig. 6. Dependence of $\Delta(1/f)$ on J^* calculated for the profiles of Fig. 5 using a J_1 Bessel function as an approximation to the wavefield $\underset{\sim}{b}$ as weighting function.

Fig. 7. Density spectrum of the low n radial modes in TCA.

Fig. 8. Simple experimental arrangement for the excitation and detection of the axisymmetric magnetoacoustic waves.

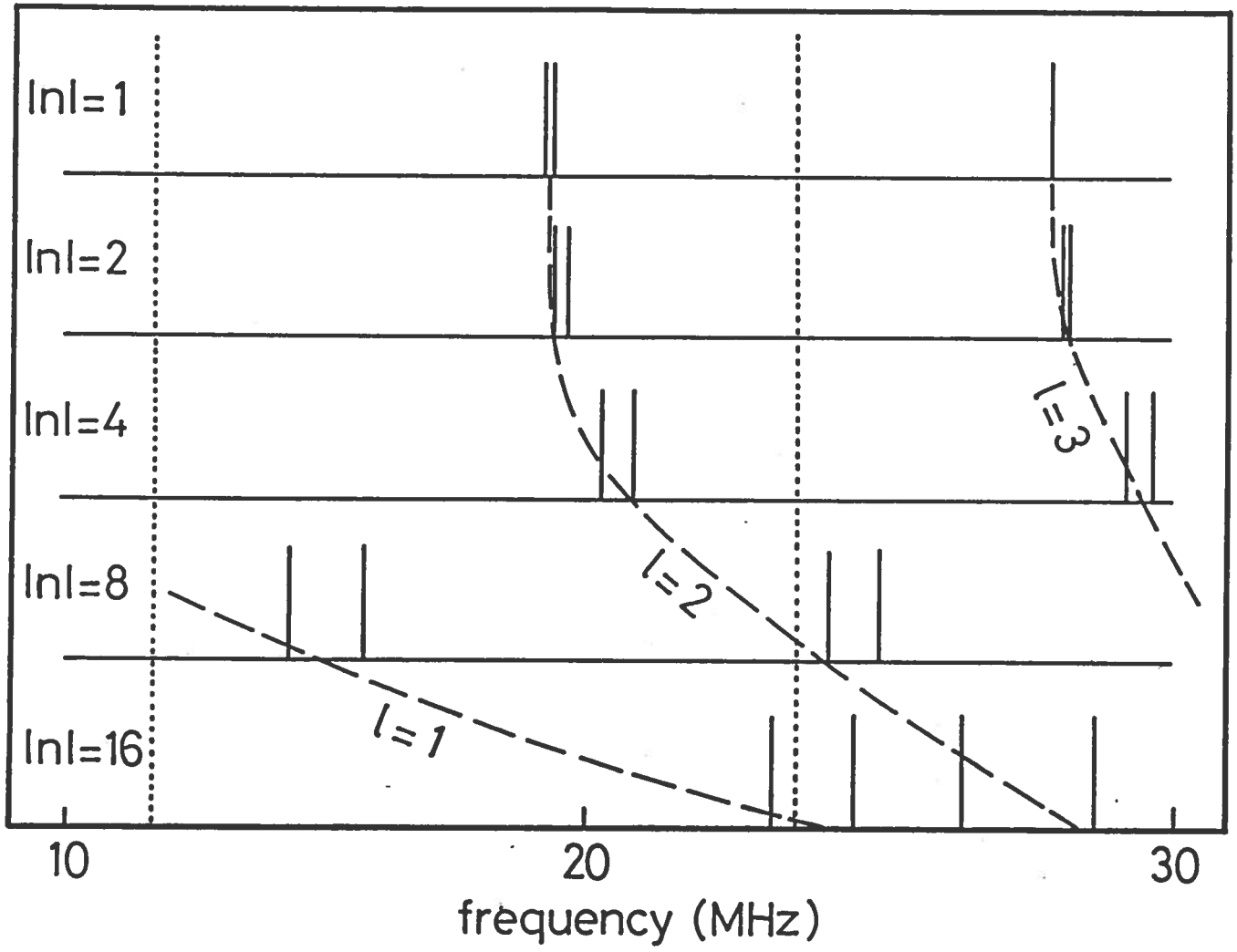

Fig. 1.

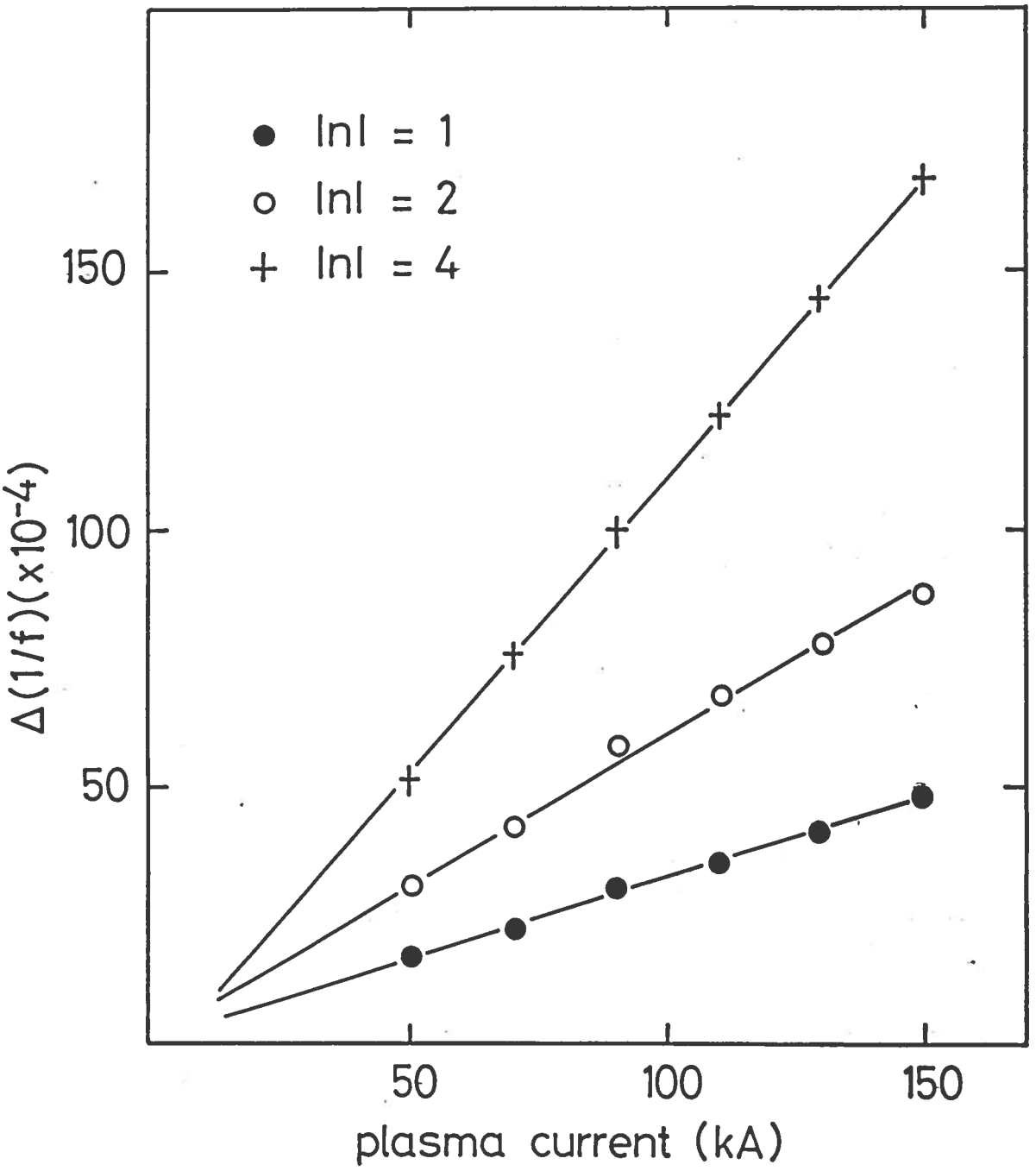

Fig. 2.

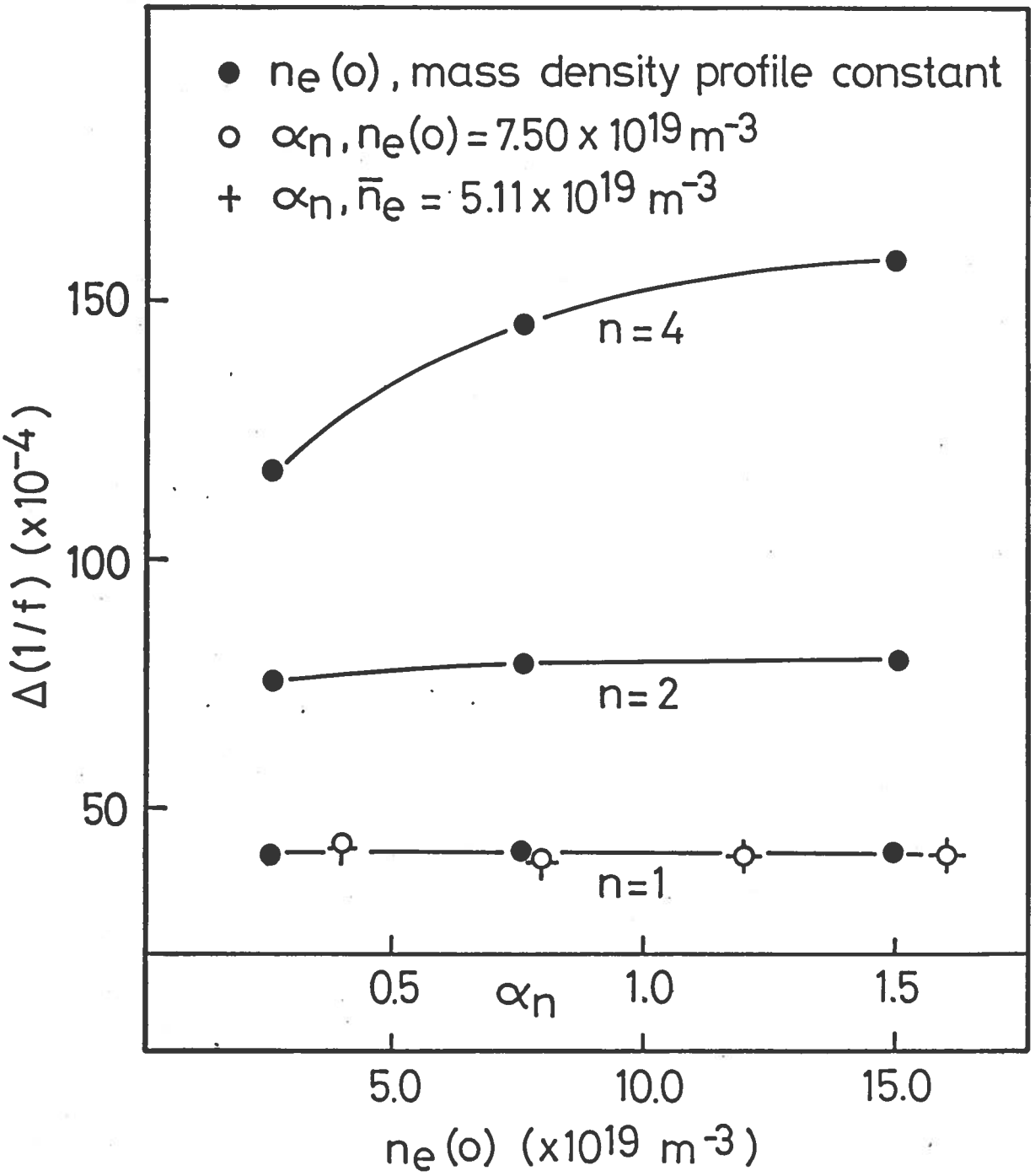
● $n_e(o)$, mass density profile constant
o α_n, $n_e(o) = 7.50 \times 10^{19}\ m^{-3}$
+ α_n, $\bar{n}_e = 5.11 \times 10^{19}\ m^{-3}$
150
100
50
$\Delta(1/f)$ $(\times 10^{-4})$
n=4
n=2
n=1
0.5
α_n
1.0
1.5
5.0
10.0
15.0
$n_e(o)$ $(\times 10^{19}\ m^{-3})$

Fig. 3.

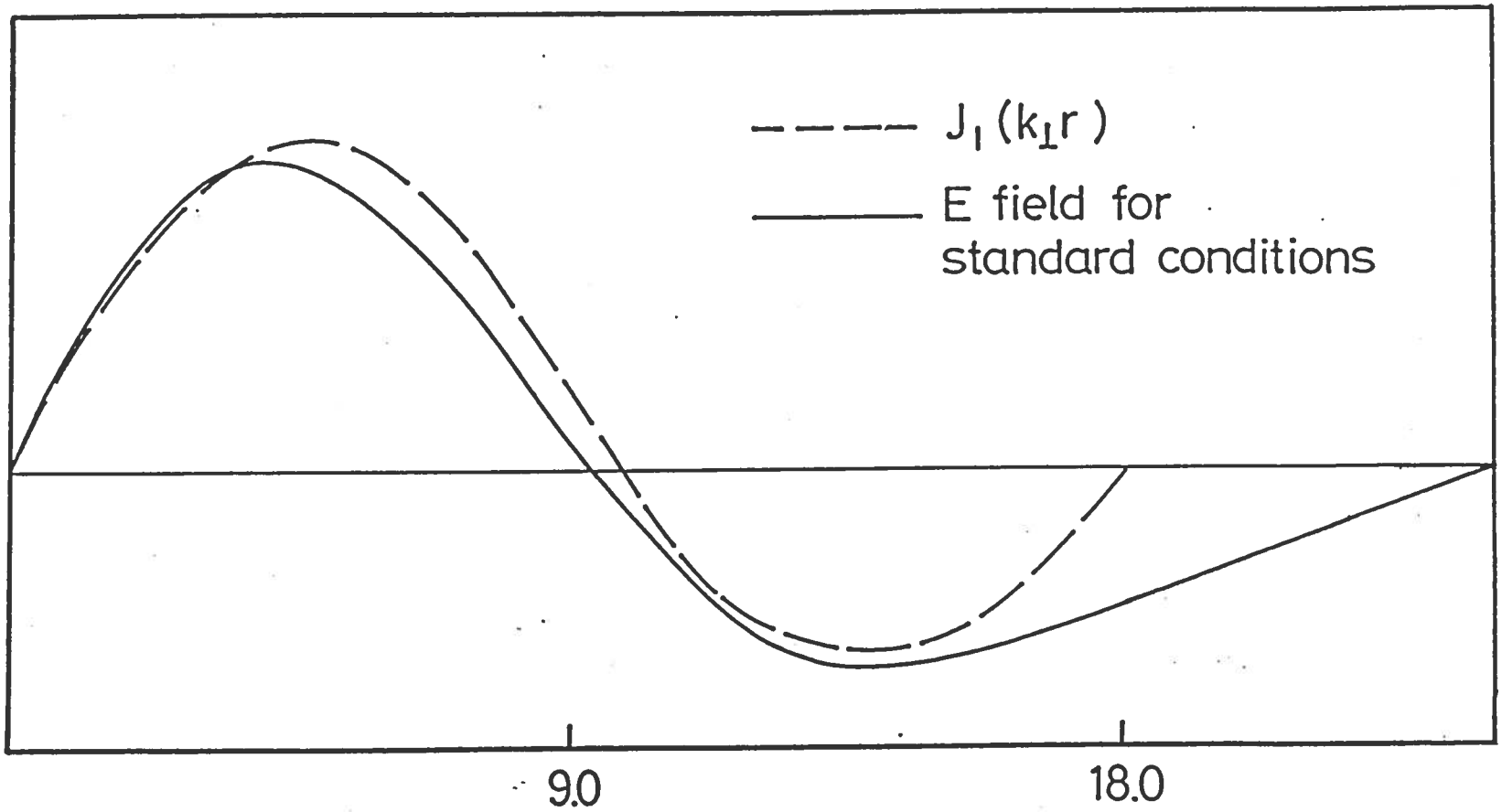
$J_1(k_\perp r)$
E field for
standard conditions
9.0
18.0
minor radius [cm]

Fig. 4.

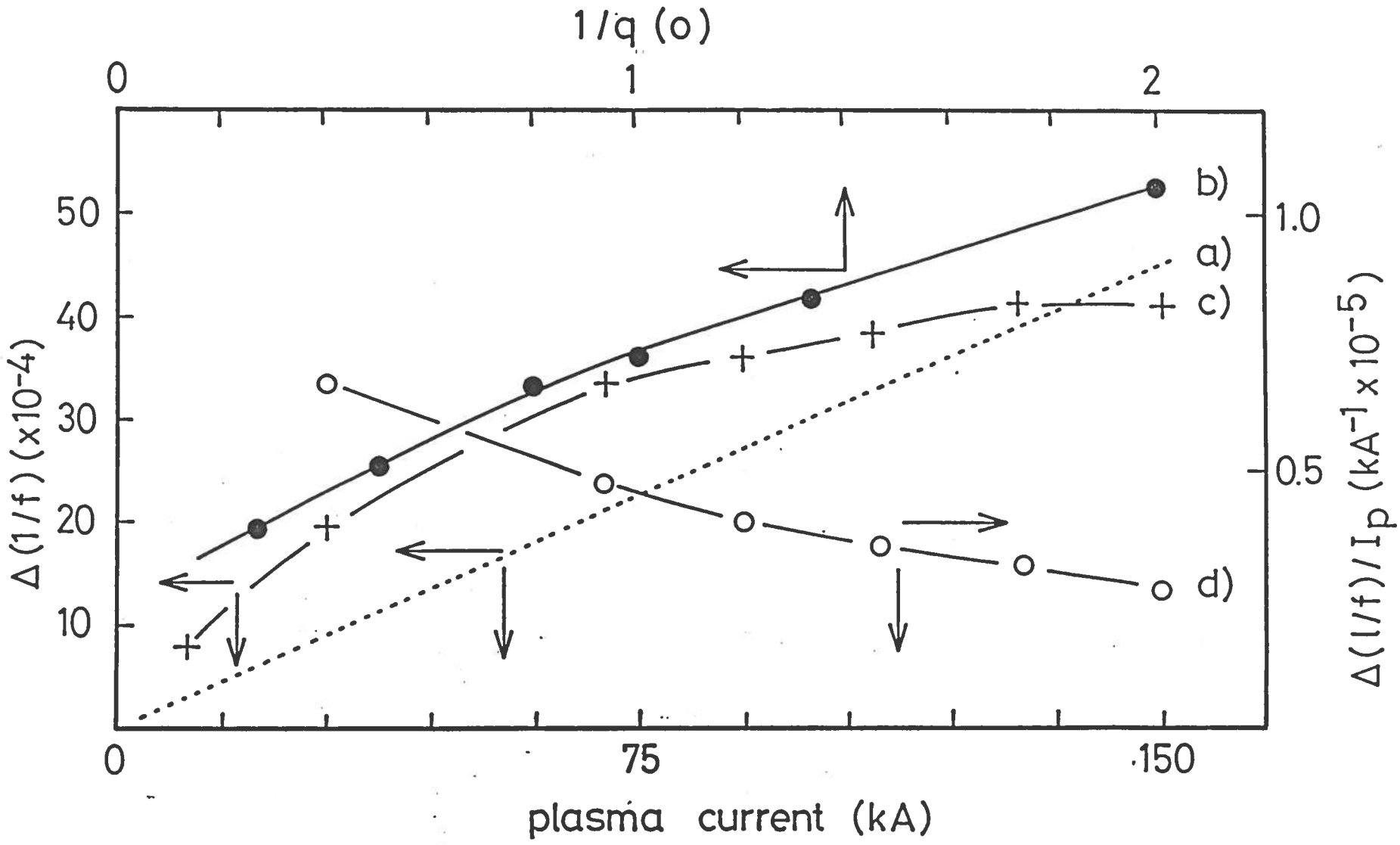
1/q (o)
0
1
2
50
40
30
20
10
Δ(1/f) (x10-4)
1.0
0.5
Δ(1/f)/Ip (kA-1 x10-5)
b)
a)
c)
d)
0
75
150
plasma current (kA)

Fig. 5.

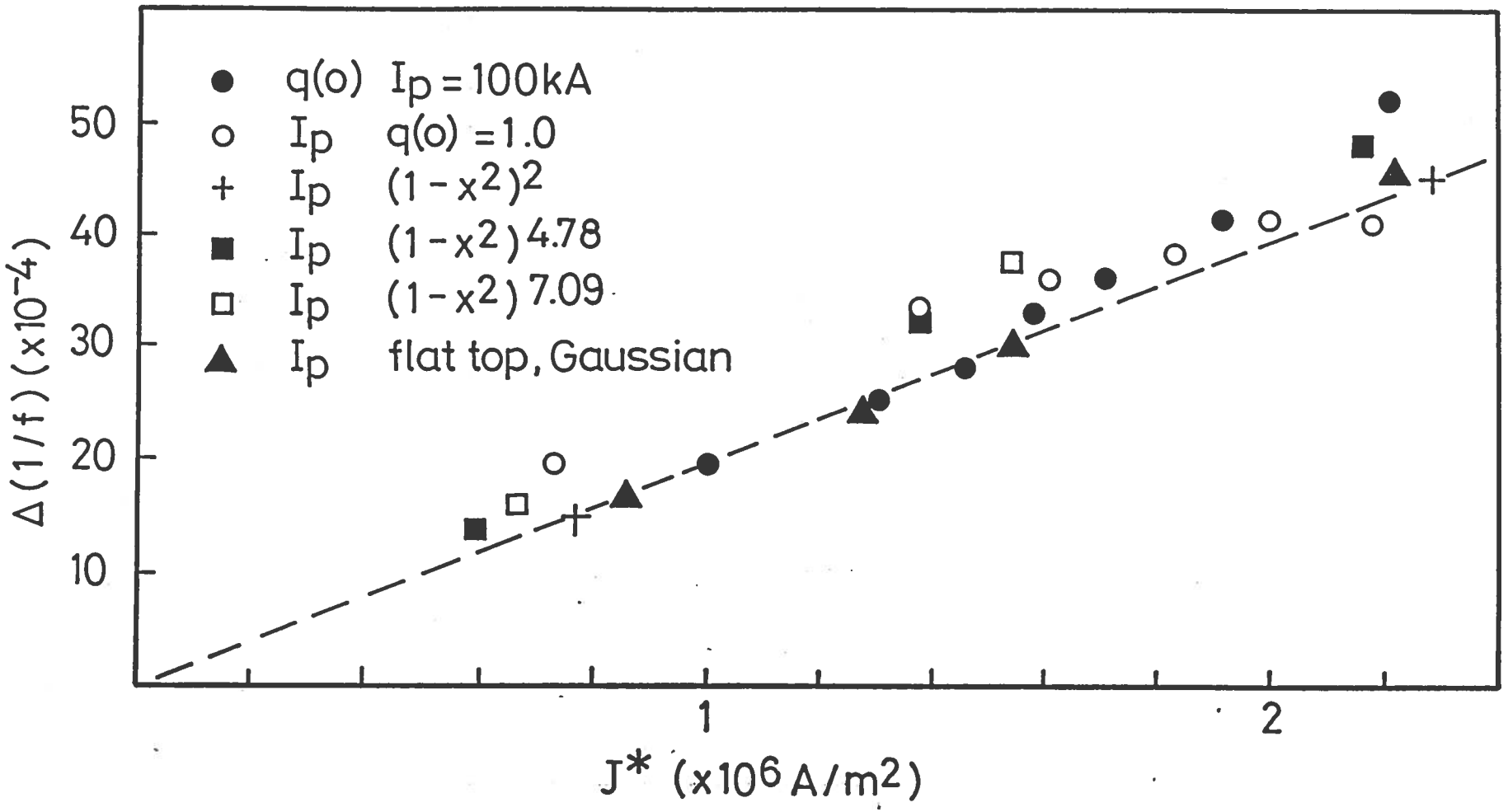
q(o) Ip = 100kA
Ip q(o) = 1.0
Ip (1 - x2)2
Ip (1 - x2) 4.78
Ip (1 - x2) 7.09
Ip flat top, Gaussian
Δ(1/f) (x10-4)
50
40
30
20
10
1
2
J* (x106 A/m2)

Fig. 6.

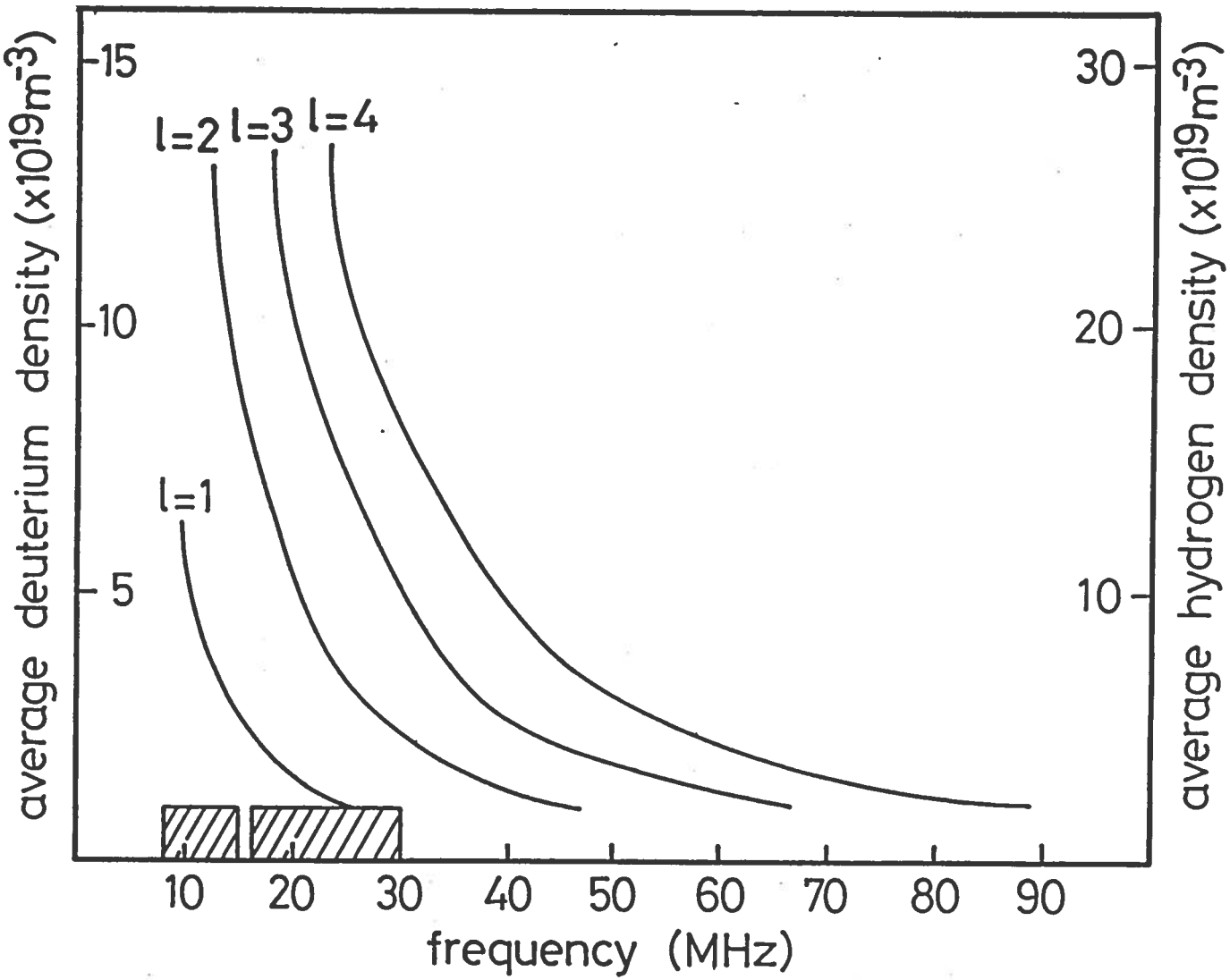
average deuterium density (x10^19m^-3)
average hydrogen density (x10^19m^-3)
15
10
5
30
20
10
l=1
l=2
l=3
l=4
10
20
30
40
50
60
70
80
90
frequency (MHz)

Fig. 7

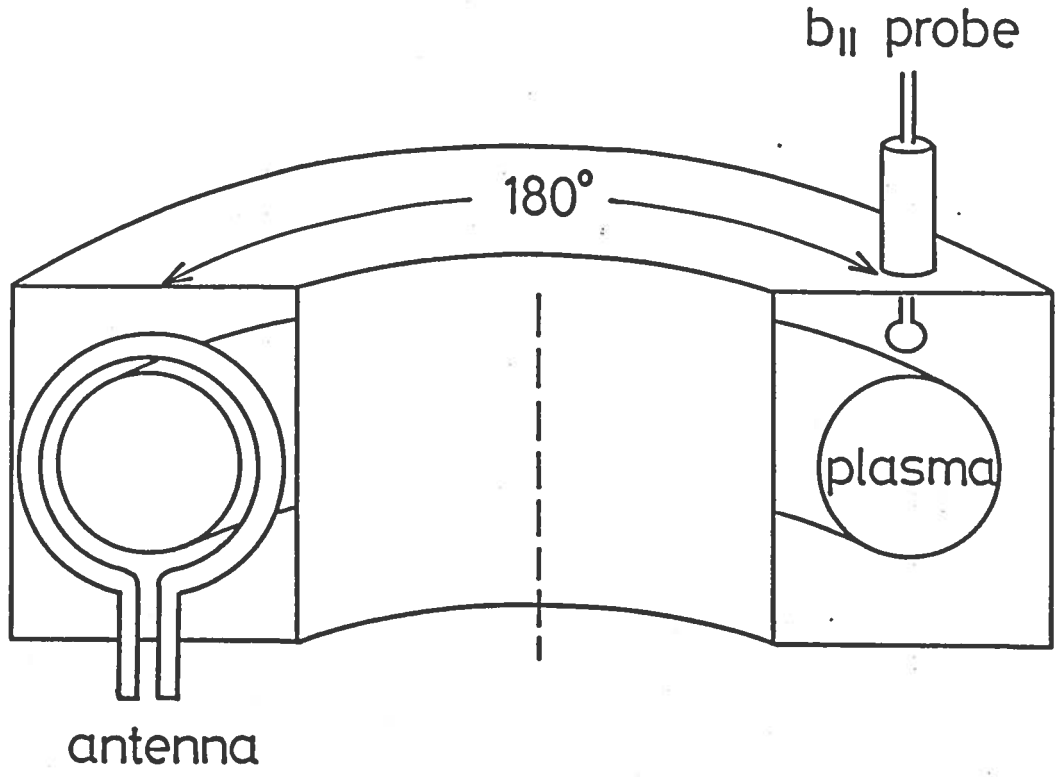

Fig. 8.